JOURNAL OF AERONAUTICAL MATERIALS
ISSN: 1005-5053
Vol. 43, Issue-01, 2023
pp. 1026-1036

GROWTH AND CHARACTERIZATION OF ZNO: SNO_2 NANOSTRUCTURES BY USING THERMAL EVAPORATION TECHNIQUE

Abdulkareem A. H[1], Q. N.Abdullah[2]
1-Department of Physics - College of Education for Pure Sciences - University of Tikrit
2-Department of Physics - College of Education for Pure Sciences - University of Tikrit

Abstract

Thin films of pure zinc oxide (ZnO) and doped with tin oxide (SnO_2) (0.3.7%wt) were prepared on glass substrates using thermal evaporation technique in vacuum at the room temperature and under low pressure (2.3×10^{-5}). The results of X-ray diagnosis of pure ZnO and doped with SnO_2 (7 wt.%) manifested that they have a mono crystalline structure, the ZnO film doped with tin oxide (3 wt.%) has a polycrystalline structure, and all films are hexagonal type. Through analysis of the resulted curves, it has become clear that the location of the peak around the angle $2\theta=34.42$ at the plane (002) is the predominant growth of the two films, the pure ZnO and doped with SnO_2 by ratio 7%. The images of the results of scanning electron microscope (FE-SEM) evinced that the pure ZnO film has the shape of stone grains and that the addition of impurities has changed the image to forms with fine sand grains, while the results of the cross section elucidated that the membrane thickness of pure zinc oxide ranges from (84 nm) to (144 nm). The optical energy gap (Eg) value of the prepared films has increased by increasing the doping ratio, and all films have a high transmittance. AFM was used to study the topography of the surfaces of prepared films and the extent to which the doping ratios affect them, showing that the rate of surface roughness decreases with increasing the doping. In order to find out the type of charge carriers, the results of the Hall Effect demonstrated that the all films are of N-type. The prepared thin films showed different responses to the gas sensing at three different operating temperatures (100, 150, and 200ºC) and the doping ratio increased the sensitivity value of the gas at an optimum temperature of 200ºC.

Keywords: Thermal evaporation, Thin films, Gas sensor, ZnO, SnO_2

1. Introduction

Numerous dangerous gases, including CO, NO_2, NH_3, CH_4, ethanol, methanol, and benzene, are routinely produced from industrial and agricultural activities on a daily basis. They are also discharged as part of automobile exhaust emissions. Others, as NO_2 and toluene, are detrimental for human health and the environment when their concentrations are above a critical threshold some of them become explosive when exposed to air, as H_2 and CH_4. It is crucial create high-precision gas sensors with in situ and real-time monitoring capabilities, as well as high sensitivity, quick response, strong selectivity, and low limit of detection (LOD) [1,2] . To improve the gas detection, high-performance gas sensors with high sensitivity, selectivity, and response speed are still needed. SnO_2, ZnO, CuO, CdO, WO_3, and TiO_2 are examples of metal oxides that can be used to identify combustible, reducing, or oxidizing gases [3]. Recently, several research teams have concentrated on nano composite materials for gas sensing applications, such as CdO-ZnO, ZnO-SnO_2, and ZnO-In_2O_3 [4,5]. Tin dioxide (SnO_2)

and zinc oxide (ZnO) are widely valuable gas sensing materials. They both are n-type materials, and their electrical conductivity depends on the density on the surface of pre-adsorbed oxygen ions. The physical and chemical characteristics of SnO_2 and ZnO are adaptable for gas sensing applications, according to their literature review. The synthesis process is another essential variable. Due to the synergistic effect between the two components, the usage of a ZnO: SnO_2 composite material is a wise decision since it modifies the properties of the materials to raise the sensitivity of metal oxide gas sensors [6]. ZnO is a significant wide-bandgap semiconductor with a direct bandgap of around ~3.37 eV. It is a material with great potential for UV nano-optoelectronic devices and lasers in the room temperature [7]. It is widely recognized that the impurity doping has a significant impact on the fundamental physical characteristics of semiconductors with certain elements, such as the electrical and optical properties, which are essential for their practical use. Numerous groups have reported the creation of doped ZnO nanoparticles and nanostructured films, and they have also investigated the characteristics of these doped nanostructures in terms of electrical, optical, and sensor functions [8–11]. The choice of material has a significant impact on the behavior of the gas sensor. When reacting with gases, the sensor's material should be conductive, especially at the semiconductor's surface component [12,13]. Zinc oxide (ZnO) and tin oxide (SnO_2) are examples of N-type materials having relatively few oxygen adsorption sites that are appropriate for sensing applications to build potential barriers. In addition, adding additives to the semiconductor material may enhance the performance of the gas sensor. Doping is the process of mixing or combining two or more materials, such as the mixed oxides of a metal, metal oxides, and polymers [14]. The advantages of composite sensors, including more thermally stable, high electron mobility, and having many hetero-contacts between the phase and the catalytic activity of sensing matrix are be able to control [12,15,16]. This research aims to study NO_2 gas sensing for pure ZnO films doped with tin oxide (SnO_2) in different ratios (0,1,3%wt). These films showed different responses to gaseous sensitization at
different operating temperatures.

2. Experimental Procedure

Thin films were obtained by vacuum thermal evaporation technique used to prepare pure ZnO thin films doped with SnO_2. They were heated in a molybdenum boat under a pressure of about (2.3×10^{-5} tors). The substrate for the boat distance was kept at 13 cm. The thin films in this study were deposited on glass bases made of glass strips with a thickness of (1 mm) and dimensions (26 x 76 mm^2) and after the process of cleaning the glass bases. Zinc powder (Zn) having a purity of 99.92% was used, doped and milled by an agate mill with the weight ratios (0, 3, and 7 wt.%) from tin (Sn) having a purity of (99.99%). Finally, the membranes were first extracted from the device after sedimentation and then placed in the furnace for thermal oxidation at a temperature of (400°C) for two hours to obtain pure zinc oxide membranes and doped with SnO_2.

3. Results and Discussions

3.1 XRD results

In order to confirm the phase structure of the produced pure ZnO thin films and anesthetic SnO_2, XRD was performed. Figure 1 shows the XRD patterns of pure ZnO and doped with

SnO_2 (3 and 7 wt.%). From the XRD pattern of pure ZnO, it can be seen that there are trend peaks of ZnO at (002) and angle (34.889◦), and that the thin film of pure zinc oxide is mono crystalline. Furthermore, the use of (3 wt.%) from SnO_2 doping steroids improved the crystalline properties. This figure also depicts that the thin film in this ratio has become polycrystalline and a SnO_2 peak appears at an angle of (41.227◦) with a direction of (210). These results were matched with the International Material Inspection Card ASTM numbered 01-075-1526 and 00-050-1429. Meanwhile, the synthesized pure ZnO reveals the crystallite size which is (15.78 nm), while the crystal size decrease with the increase of doped [19, 20, 21].

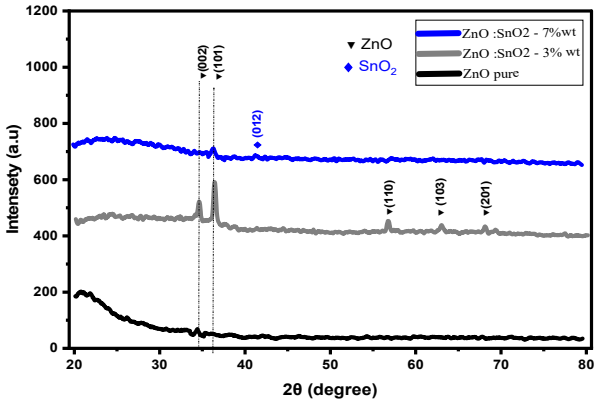

Fig. 1: The XRD patterns of ZnO:SnO_2 (0, 3 and 7 wt.%) deposited by thermal evaporation in vacuim

3.2 AFM results

The morphology for the surface of pure ZnO and doped with SnO_2 thin films, which were prepared at various concentrations and deposited on the glass substrate at the RT, has been analyzed by AFM. The three-dimensional topographic views of AFM images for these films are displayed in Fig. 2. The AFM images revealed that the doped rate has a strong impact on the surface morphology. The films also appeared a homogeneous surface made of pyramidal granules with sharp edges. The roughness of the ZnO pure film was measured to be (701.9 nm). The average roughness and particle diameter and (RMS roughness) decreased with an increase of doped (SnO_2), while the surface roughness rate decreased to (100 nm) at 7 wt.% doped for SnO_2, and the diameter size of this ratio was about (5 nm) [22]. This is due to the rearrangement of the atoms in the film.

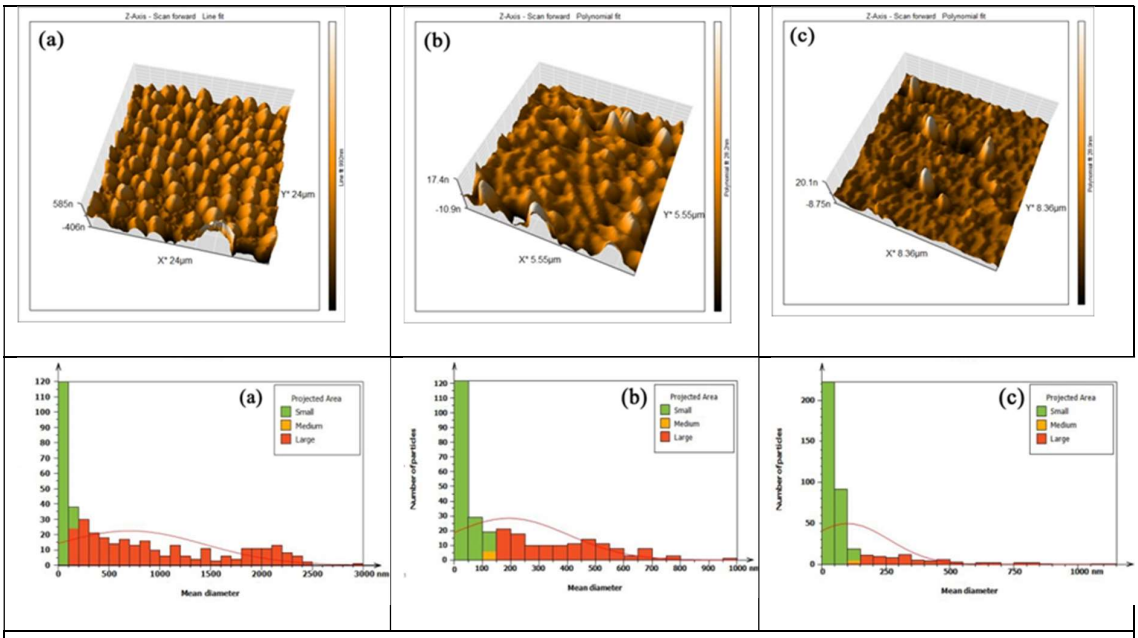

Fig. 2: Surface morphology for pure ZnO films doped with SnO_2 (0, 3, and 7 wt.%, respectively) deposited by thermal evaporation in vacuim

3.3. FE-SEM results

The FE-SEM images of the ZnO thin films (doped and undoped) prepared by the method of thermal evaporation in vacuum are presented. Figure.3(a) shows the cross-sectional image of the membrane thickness of the pure zinc oxide sample with the highest membrane diameter at (~144 nm). The SEM images of pure ZnO depict that the nanocomposite films are in the form of medium-sized sandstones, as in Fig.3(b), where the grain distribution diagram reveals that the sizes of these nanoparticles range is (~ 30-80 nm). And, the SEM images of ZnO films doped with 3 %wt SnO_2 display the dispersed agglomerated nanoparticle-like morphology, as in Fig. 3 (c). Also, the SEM images manifest that the nature of their composition is influenced by the technique used in the preparation of these thin films and different shapes appear in each work. Overall, the thinfilm doped with (7 %wt) SnO_2 evinced more smoothness for nanoparticles and had fine agglomerates, as shown in the fig.3 (d) [23, 24]. The elemental composition was confirmed by energy X-ray dispersive spectroscopy (EDS). Figure. 4(a, b, and c) elucidates that the tin, zinc and oxygen are the main parts of the spectrum. These ingredients indicate their strength according to their percentage appears in a film. However, in Fig.4(a and c), there are two major unlabeled peaks at the lower end. Those peaks at the lower end correspond to the carbon (C) and silicon (Si). The percentage of tin in the composite sample increases for the simples (b, c), and it is observed that in Fig. 4 with the change in composition, the morphology of the sample changes accordingly [25].

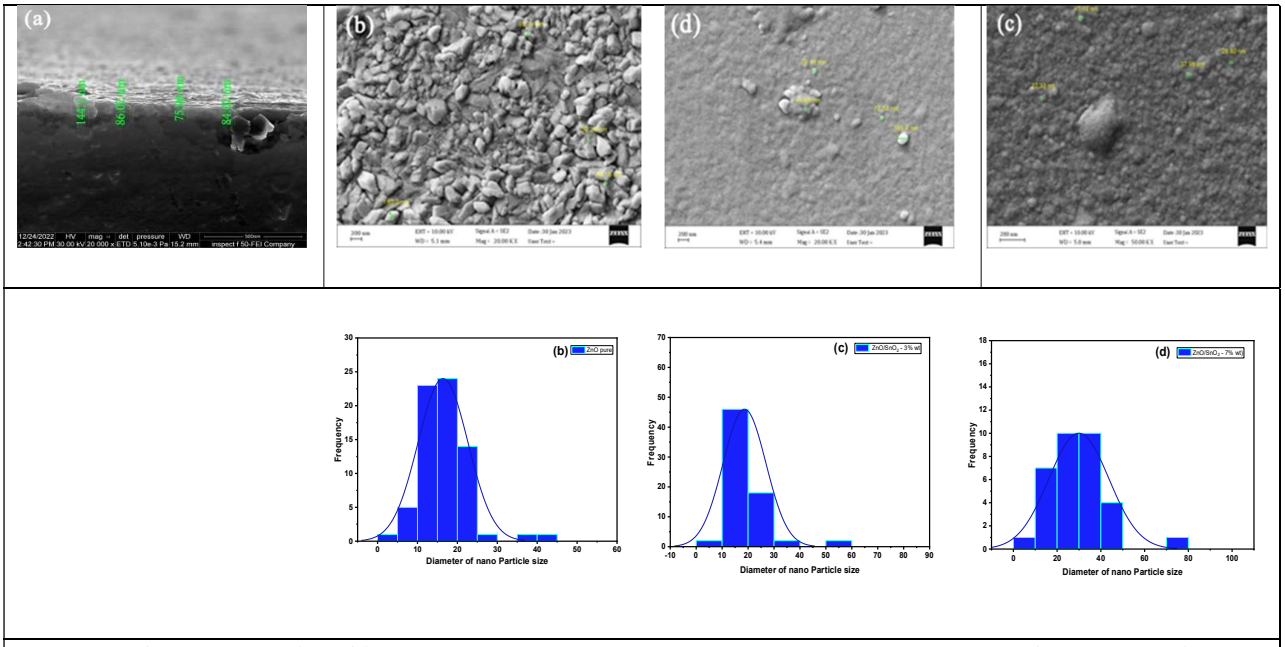

Fig. 3 (a) the cross-sectional image **of pure ZnO film and fig. 3(b,c,d respectively)** the FE-SEM images of the ZnO thin films **doped with SnO_2 (0, 3, 7 %wt) and deposited by thermal evaporation in vacuim**

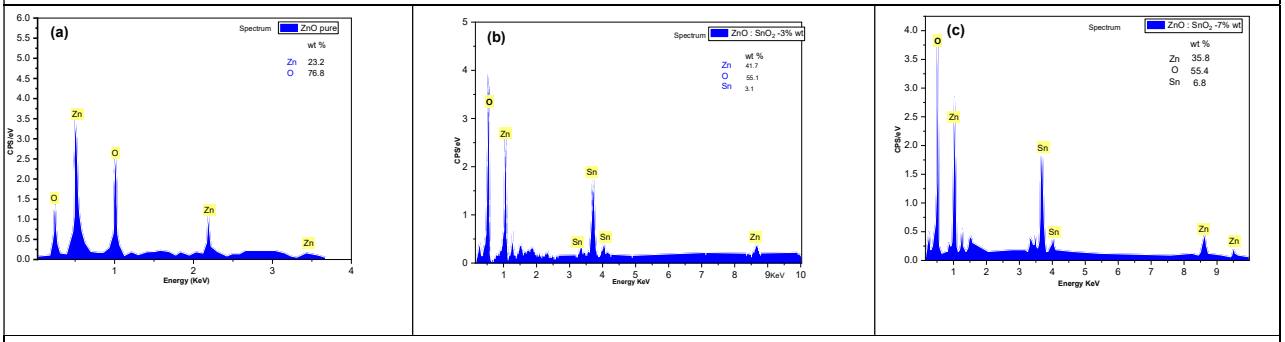

Fig. 4(b,c,d respectively) The EDX spectrum of pure ZnO thin films doped with SnO_2 (0, 3, and 7 %wt) and deposited by thermal evaporation in vacuim

3.4 Optical properties results

The optical properties of thin films of pure ZnO and SnO_2 doped (0, 3, and 7 % wt) have been studied in different weight ratios and deposited by thermal evaporation technique in vacuum, as these properties have a major role in determining the importance of membranes in their use as a gas sensor. Using the following equation, the absorption coefficient at the frequency associated with the high absorption region can be easily calculated from the absorption (A) and the film thickness (t):

$$a = 2.303\ A/t$$

Spectra of crystalline and amorphous materials' fundamental absorption edge have an important property. To determine the material band gap, it is necessary to know the transition from valence to conduction band. The energy band gap (Eg) was calculated [26].

$$\alpha h\upsilon = B(h\upsilon - E_g)^r$$

Where, B is a structure-dependent constant, Eg is the optical energy gap, and r is an index defining the optical absorption process that can take a value of 1/2, 3/2, 2, or 3 depending on the sort of electronic transition that causes the absorption to take place [27,28]. On the basis of UV-Vis spectra, the values of the absorption coefficient for each wavelength of electromagnetic radiation were obtained. The value 0.5 was chosen for the r-coefficient, which corresponds to each allowed direct optical transition

The absorption spectrum was calculated as a function of wavelength, as the absorption spectrum shown in Fig.5(a) demonstrates a gentle opposite behavior to transmittance due to the logarithmic relationship between them, as the absorption of membranes decreases with increasing doping SnO_2 with increasing wavelength owing to the low energies of incident photons and their inability to raise electrons from the valence band to the conduction band, as the relationship is inverse between the wavelength and the energy of the photon [29]. Figure.5(b) appears that the transmittance spectrum of the prepared membranes in different proportions is a function of wavelength, as the all precipitated membranes have an optical transmittance of (95-98%) in the range of wavelengths (400-1100 nm). The high transparency and sharp edge of absorption at (398 nm) indicate the high optical quality of pure ZnO thin film and doped SnO_2 by weight ratios (0, 3, and 7%wt). The transmittance illustrates the opposite behavior to the absorption spectrum due to the logarithmic relationship between them, where it increases with increasing the percentage of distortion [30]. As it is known, the absorption spectrum of zinc oxide is within the ultraviolet (UV) spectrum region, so the wavelength range (440-498 nm) has been determined because this range is where the basic absorption process occurs [31]. Fig.5(c) shows the plot of $(\alpha h\upsilon)^2$ versus photon energy for the films under investigation. One can see that the calculated optical energy gap for the undoped ZnO was found to be a round ~3.26 eV. The band gap value of 3 wt.% tin oxide (SnO_2) doped was increased to 3.78 eV, whereas the further increase in the SnO_2 - 7 wt.% resulted in an increase in the band gap value up to 3.82 eV [23, 33].

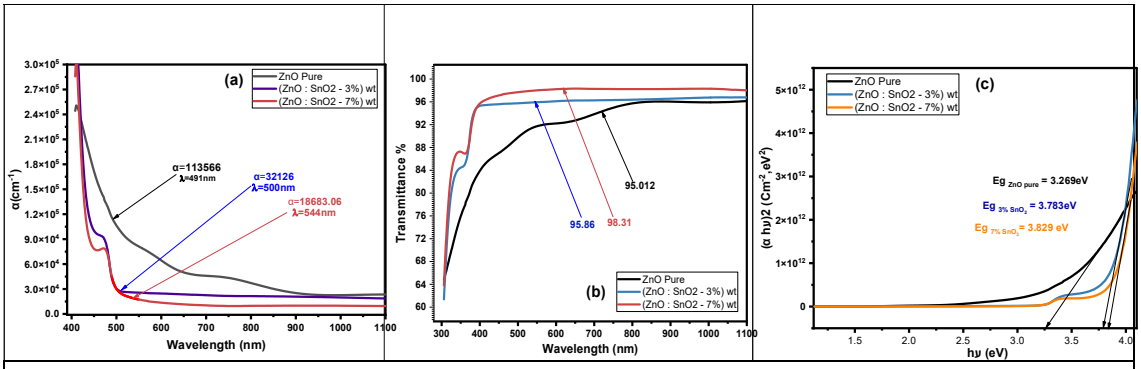

Fig. 5(a,b,c) The optical properties of pure ZnO thin films doped with SnO_2 (0, 3, and 7 %wt) and deposited by thermal evaporation in vacuum

4. Electrical Properties results

The study of the electrical properties of ZnO: SnO_2 (0,3,7% wt) thin films prepared by vacuum thermal evaporation has gained a great importance in determining their behavior for use in various applications such as a gas sensor, for example. Figure. 6(a,b,c) views the current-

voltage (I-V) properties of pure zinc oxide and doped SnO_2 precipitated on glass substrate, and it has been found that the films exhibited Ohmic behavior at low voltages. The current increases with increasing voltages in the front and reverse biases and it is almost the same in the biases. But, the intensity of illumination 0.3 Watt on the membrane has a small effect, as it is clear through the drawings. And, it is also noted through the sample doped with SnO_2 by (3% wt) that in the case of darkness, the current is stable and constant with increasing voltages. But at the appropriate light intensity with the temperature falling with the light, it worked to change its behavior in the dark, the increase in voltages increased the current, except for the (7% wt) impurity rate, which had a difference in behavior, which increased the ideal factor, and the voltage barrier decreased and increased Spending Agent.

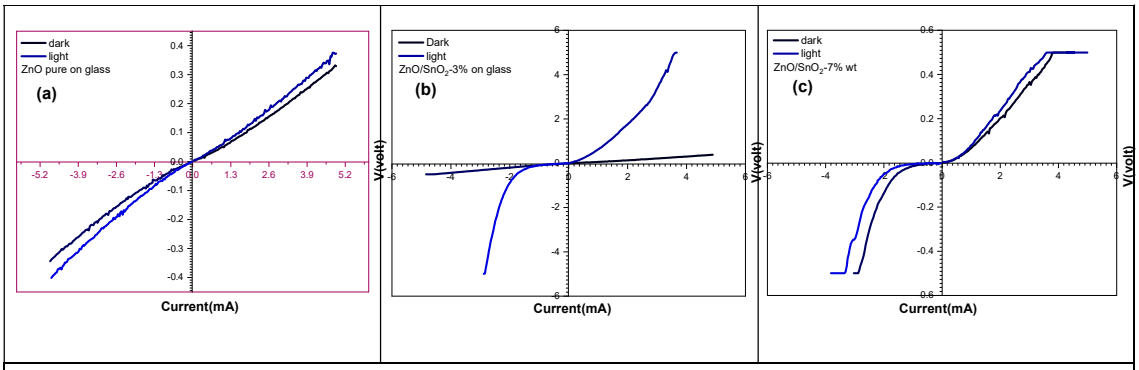

Fig. 6(a,b,c) The current-voltage(I-V) properties of pure zinc oxide and doped SnO_2 (0, 3,7 %wt) precipitated on glass

5. Gas Sensor Result

The ZnO:SnO_2 gas sensors were fabricated on glass by thermal evaporation in vacuum technique. Using a homemade testing setup, the ability of ZnO: SnO_2 (0,3,7%wt) sensors to detect gases was studied. Using a Keithley 2602A source ammeter system, the change of sensor resistance was observed through a continuous recording. The response (S) of sensors is defined as S = Rg/Ra (for oxidizing gas), where Ra and Rg are the resistances in air and test gas, respectively, used to describe the response (S) of sensors. The recovery time is the amount of time needed to restore 90% of the initial resistance, whereas the response time is commonly defined as the time needed to attain 90% of the steady response signal ZnO:SnO_2 NPs sensors that show their best performance at a temperature of 200°C. As a result, the ZnO:SnO_2 composite's gas-sensing capabilities employing oxidizing gas fast increase the selectivity of sensors. Figure.7 (a,b,c) manifests the response time and the retrieval time for pure ZnO due to the change of resistance with time at three different temperatures of un doped zinc oxide film as well as the transient response of the pure ZnO film sensors toward 1.6 ppm NO_2 at 100°C and 1.48 ppm NO_2 at 200°C. The gas sensing of this sample was the best result at a temperature of 100°C, S = ~85% with a response time of (16 sec), and a recovery time of (14 sec). Figure 7(d,e,f) evinces that the sensors' reaction quickly rises in response to the NO_2 concentration. This outcome is the consequence of more NO_2 molecules interacting with the NPs sensors. At temperatures between 100°C and 200°C, the gas responses of ZnO: SnO_2 (3 wt.%) sensors reach the highest values S = 2943%, the response was (9 sec) and the recovery time was (14

sec) at 200°C [35 ,34]. At 200°C, the ZnO: SnO_2 (7 wt.%) sensors, Fig. 7(g, h, and k) demonstrates a greater response than pure ZnO sensors that are not doped with SnO_2; the gas response of the ZnO: SnO_2 (7 wt.%) sensors ranges from S=165% to S=535% at 150 and 200°C, respectively. Due to the connection between ZnO and SnO_2, which enables the electrons to transfer readily across the interface between two materials, the ZnO: SnO_2 thin films doping (0,3,7 % wt) sensors have a high response rate. As a result, when exposed to the target gas, the HJs are simple to modify. When the working temperature increases from 100°C to 200°C, the resistance of the sensor rapidly decreases. The resistance of SMO materials normally varies with temperature, and at higher temperatures, the semiconductor electrons become more mobile. Therefore, the ZnO: SnO_2 doping (3 and 7 wt.%) still elucidates higher resistance than pure ZnO [36].

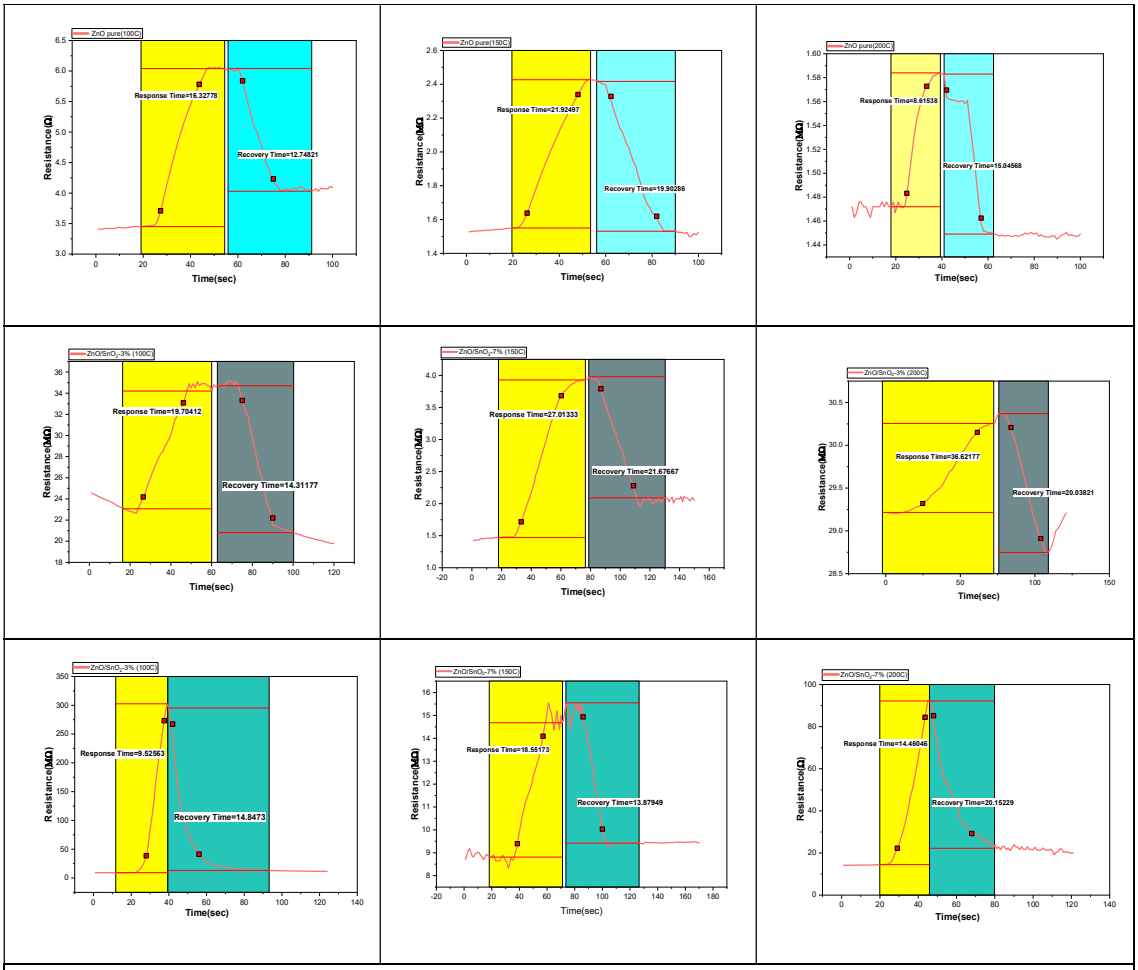

Fig. 7: The response and recovery time at different operating temperatures (100, 150, and 200°C) for pure ZnO thin films and doped with SnO_2 (0, 3, and 7% wt) and deposited by thermal evaporation in vacuum

6. Conclusion

This work demonstrated the use thermal evaporation method in synthesizing ZnO :SnO_2 (0,3,7%wt) films nanostructures for gas sensing applications. The performance of the various

nanostructures for gas sensing was examined and compared using ZnO:SnO_2 films. Comparative gas sensing experiments revealed that ZnO:SnO_2 films perform better than other materials, which may be ascribed to the materials' high porosity, increased number of active sites, and incorporation of core-outer junctions. ZnO:SnO_2 nanostructures that have been created thus far have a lot of potential for use in gas sensor applications. Additionally, the synthesis of additional nanostructures based on metal oxide materials, such as SnO_2:ZnO, In_2O_3:SnO_2, ZnO, WO_3, and ZnO:TiO_2, may be accomplished using the method provided by this study.

References

]1[M. Jerrett, D. Donaire-Gonzalez, O. Popoola, R. Jones, R. C. Cohen, E. Almanza, A. de Nazelle, I. Mead, G. CarrascoTurigas, T. Cole-Hunter, M. Triguero-Mas, E. Seto and M. Nieuwenhuijsen, Environ. Res., 158 (2017) 286–294 .

[2]Z. A. Barakeh, P. Breuil, N. Redon, C. Pijolat, N. Locoge and J.-P. Viricelle, Sens. Actuators, B, 2017, 241, 1235–1243 .

[3] Batzill M. and Diebold U., 2005, Prog. Surf. Sci., 79, 47.

[4]Sharma A. K., Potdar S. S., Pakhare K. S., Patil U. M., Patil V. S. and Naik M. C., 2020, J. Mater. Sci.: Mater. Electron, 31, 1.

[5]Zhang K., Qin S., Tang P., Feng Y. and Li D., 2020, J. Hazard. Mater., 391, 122191.

[6]Wang C., Yin L., Zhang L., Xiang D. and Gao R., 2010 Sensors, 10, 2088.

[7]M. H. Huang, S. Mao, H. Yan, Y. Wu, H. Kind, E. Weber, R. Russo, and P. Yang, Science, 292 (2002) 1897.

[8]C. H. Jung, D. J. Kim, Y. K. Kang, and D. H. Yoon, Thin Solid Films, 517 (2009) 4078.

[9]E. Pa´l, V. Hornok, A. Oszkoo´, and I. De´ka´ny, Coll. Surf. Sci A: Physicochem. Eng. Aspects, 340 (2009) 1.

[10]C. H. Ahn, S. K. Mohanta, B. H. Kong, and H. K. Cho, J. Phys. D: Appl. Phys., 42 (2009) 115106.

[11]P. K. Sharma, R. K. Dutta, A. C. Pandey, S. Layek, H. C. Verma, and J. Magn. Magn. Mater., 321 (2009) 2587.

[12]Korotcenkov G., 2007, Metal oxides for solid-state gas sensors: What determines our choice? Materials Science and Engineering: B 139 1-23 .

[13]Wang C., Yin L., Zhang L., Xiang D. and Gao R., 2010, Metal oxide gas sensors: Sensitivity and influencing factors Sensors, 10 2088-106.

[14]Singh N., Ponzoni A., Comini E. and Lee P. S., 2012, Chemical sensing investigations on Zn–In2O3 nanowires Sensors and Actuators B: Chemical, 171–172 244-8 .

[15]Yu J. H. and Choi G. M., 1999, Electrical and CO gas-sensing properties of ZnO/SnO2 heterocontact Sensors and Actuators B: Chemical, 61 59-67 .

[16]Haeng Yu J. and Man Choi G., 1998 Electrical and CO gas sensing properties of ZnO–SnO2 composites Sensors and Actuators B: Chemical, 52 251-6.

[17]da Silva, L. F., M'peko, J. C., Catto, A. C., Bernardini, S., Mastelaro, V. R., Aguir, K., and Longo, E., (2017), UV-enhanced ozone gas sensing response of ZnO-SnO_2 heterojunctions at room temperature, Sensors and Actuators B: Chemical, 240, 573-579.

[18]Huang, X., Shang, L., Chen, S., Xia, J., Qi, X., Wang, X., and Meng, X. M., (2013), Type-II ZnO nanorod–SnO2 nanoparticle heterostructures: Characterization of structural, optical and photocatalytic properties. Nanoscale, 5(9), 3828-3833.

[19] Aadim, K. A., and Essa, M. A., (2019), Structural and Optical properties of SnO2 doped ZnOthin films prepared by Pulsed Nd: YAG Laser Deposition. Journal of College of Education, 3(3.(

[20]S. K. Sinha, R. Bhattacharya, S. K. Ray and I. Manna, Influence of deposition temperature on structure and morphology of nanostructured SnO_2 films synthesized by pulsed laser deposition, Materials Letters, Vol. 65 , Issue 2, pp. 146-149, 2011.

[21]Zarei, S., Hasheminiasari, M., Masoudpanah, S. M., and Javadpour, J., (2022), Photocatalytic properties of ZnO/SnO_2 nanocomposite films: Role of morphology. Journal of Materials Research and Technology, 17, 2305-2312.

[22]Mu, S., Wu, D., Qi, S., and Wu, Z., (2011), Preparation of polyimide/zinc oxide nanocomposite films via an ion-exchange technique and their photoluminescence properties. Journal of Nanomaterials, 2011, 1-10.

[23] Singh, A., Sikarwar, S., and Yadav, B. C., (2021), Design and fabrication of quick responsive and highly sensitive LPG sensor using ZnO/SnO2 heterostructured film., Materials Research Express, 8(4), 045013.

[24]E. A. Davis, and N. F. Mott, Conduction in non-crystalline systems V. Conductivity, optical absorption and photoconductivity in amorphous semiconductors, Philos. Mag., 22 (1970) 903–922.

[25] H. Hou, Z. Jun, A. Reuning, A. Schaper, J. H. Wendorff, and A. Greiner, Macromolecules, 35 (2002) 2429.

[26]G. Ma, D. Yang, and J. Nie, Preparation of porous ultrafine polyacrylonitrile (PAN) fibers by electrospinning, Polym. Adv. Technol. 20 (2) (2009) 147–150.

[27]S. T. Tan, B. J. Chen, X. W. Sun and W. J. Fan, Blue shift of optical band gap in ZnO thin films grown by metal-organic chemical-vapor deposition', Journal of Applied Physics Vol. 98, p. 13505 (2005).

[28] Norbert H. Nickel and Evgenii Terukov, Zinc Oxide - A Material for Micro- and Optoelectronic Applications, Springer, (2005.(

[29]Periasamy, C., Prakash, R., and Chakrabarti, P., (2010), Effect of post annealing on structural and optical properties of ZnO thin films deposited by vacuum coating technique, Journal of Materials Science: Materials in Electronics, 21, 309-315.

[30]Martínez, D. T., Pérez, R. C., Delgado, G. T., and Ángel, O. Z., (2012), Structural, morphological, optical and photocatalytic characterization of ZnO–SnO2 thin films prepared by the sol–gel technique., Journal of Photochemistry and Photobiology A: Chemistry, 235, 49-55.

[31] Rashad, M. M., Ismail, A. A., Osama, I., Ibrahim, I. A., and Kandil, A. H. T., (2014), Photocatalytic decomposition of dyes using ZnO doped SnO2 nanoparticles prepared by solvothermal method, Arabian Journal of Chemistry, 7(1), 71-77.

[32]Duoc, V. T., Hung, C. M., Nguyen, H., Van Duy, N., Van Hieu, N., and Hoa, N. D., (2021), Room temperature highly toxic NO_2 gas sensors based on rootstock/scion nanowires

of SnO_2/ZnO, ZnO/SnO_2, SnO_2/SnO_2 and, ZnO/ZnO, Sensors and Actuators B: Chemical, 348, 130652.

[33] Zhao, S., Shen, Y., Maboudian, R., Carraro, C., Han, C., Liu, W., and Wei, D., (2021), Facile synthesis of ZnO-SnO_2 hetero-structured nanowires for high-performance NO_2 sensing application. Sensors and Actuators B: Chemical, 333, 129613.

[34]M. M. Arafat, B. Dinan, S. A. Akbar, and A. S. M. A. Haseeb, Gas sensors based on one dimensional nanostructured metal-oxides: A review, Sensors, 12, (2012), 7207–7258, https://doi.org/10.3390/s120607207.